EUROFUSION WPJET2-PR(16) 14813

N Catarino et al.

Assessment of Erosion, deposition and fuel retention in the JET-ILW divertor from Ion Beam Analysis data

Preprint of Paper to be submitted for publication in
22nd International Conference on Plasma Surface Interactions
in Controlled Fusion Devices (22nd PSI)

This work has been carried out within the framework of the EUROfusion Consortium and has received funding from the Euratom research and training programme 2014-2018 under grant agreement No 633053. The views and opinions expressed herein do not necessarily reflect those of the European Commission.

Assessment of Erosion, deposition and fuel retention in the JET-ILW divertor from Ion Beam Analysis data

N. Catarino[a], N. P. Barradas[b], V. Corregidor[a], A. Widdowson[c], A. Baron-Wiechec[c], J. P. Coad[c], K. Heinola[d], M Rubel[e], E. Alves[a] and JET Contributors*

EUROfusion Consortium, JET, Culham Science Centre, OX14 3DB, Abingdon, UK

[a] *IPFN, Instituto Superior Técnico, Universidade de Lisboa, 1049-001, Lisboa, Portugal*

[b] *C^2TN, Instituto Superior Técnico, Universidade de Lisboa, E.N. 10, Sacavém 2686-953, Portugal*

[c] *Culham Centre for Fusion Energy, Culham Science Centre, Abingdon, OX14 3DB, UK*

[d] *University of Helsinki, P.O. Box 64, 00560 Helsinki, Finland*

[e] *Royal Institute of Technology, Association EURATOM-VR, SE-100 44 Stockholm, Sweden*

[*] *See the Appendix of F. Romanelli et al., Proceedings of the 25th IAEA Fusion Energy Conference 2014, Saint Petersburg, Russia*

Abstract

Post-mortem analyses of individual components provide relevant information on plasma-surface interactions like tungsten erosion, beryllium deposition and plasma fuel retention into divertor tiles via implantation or co-deposition. Ion Beam techniques are ideal tools for such purpose and have been extensively used for post-mortem analyses of selected tiles from JET following each campaign.

In this contribution results from tiles removed from JET ITER-Like Wall (JET-ILW) divertor following the 2013-2014 campaign are presented. The results summarize erosion, deposition and fuel retention along the poloidal cross section of the divertor surface and provide data for comparison with the first JET-ILW campaign, showing a similar pattern of material migration.

PACS: 52.40.Hf, 28.52.Fa

PSI-20 keywords: JET, ITER-like wall, plasma facing components, erosion, deposition, Ion beam analysis

*Corresponding author address: IFPN/LATR, Instituto Superior Técnico (IST), Universidade de Lisboa, Estrada Nacional Nº 10, km 139,7, 2695-066 Bobadela, Portugal

*Corresponding author E-mail: norberto.catarino@ctn.tecnico.ulisboa.pt

Presenting author: Norberto Catarino

Presenting author email: norberto.catarino@ctn.tecnico.ulisboa.pt

1. Introduction

The future of fusion reactors will depend on the behaviour of the materials used in Plasma Facing Components (PFCs) which will determine their lifetime and also influence retention of hydrogen isotopes in the vessel. Among other processes, erosion of PFCs and subsequent re-deposition are critical for the operation of fusion devices and must be properly understood. Erosion mainly occurs by sputtering due to the plasma ions with energies up to several keV and impact of neutral particles and determines the lifetime of PFCs in fusion devices. The eroded material subsequently undergoes re-erosion/re-deposition until it is deposited onto remote areas and no longer interacts with the plasma. The co-deposition of fuel particles with erosion products leads to an increase in the tritium inventory.

During the 2013-2014 JET-ILW campaign several marker tiles were installed in the main chamber and divertor to assess the global picture of erosion and re-deposition processes occurring during machine operation [1–3]. The divertor is the region where these processes are expected to occur at extreme conditions and post mortem analysis offers the possibility to unveil some of the major effects.

Fuel inventory, material erosion and melting have a major impact on the performance of the divertor. A large number of diagnostic tools have been used to study these phenomena. This study presents the results from Ion Beam Analysis (IBA) techniques such as Rutherford Backscattering Spectrometry (RBS) and Nuclear Reaction Analysis (NRA) for fuel retention and erosion patterns in JET. The results give information on the processes occurring at the inner and outer divertor corners as well as at the transition from the inner main chamber wall (high field side) and the inner divertor.

2. Experimental Details

A Selection of passive diagnostic components and marker tiles were installed in the JET chamber for the 2013-2014 campaign. The tile numbers and location in the divertor are shown in Figure 1. In this work, results for divertor Tiles 1, 4 and 6, are presented, discussed and highlighted. The tiles are solid structures where the plasma facing surface is shaped with flat segments at different angles. This

introduces some difficulties in mounting of the tile which were overcome by measuring each of the flat segments separately, i.e. the tile was mounted in the chamber several times using specially designed holders to orient each surface perpendicular to the ion beam as shown in Figure 2. All positions on divertor tiles are located using the s-coordinate system (Figure 1), starting at the upper left corner of the High Field Gap Closure tile (Tile 0) and following the tile surfaces from the inner to the outer divertor.

The divertor tiles, with the exception of Tile 5, consist of CFC coated with 10 to 20 μm tungsten (W) on the plasma-facing surfaces[4,5]. Marker tiles, like Tile 1, used to study erosion and deposition in the divertor were coated with a W marker layer with a thickness of about 3 μm with a 3 μm thick molybdenum (Mo) interlayer between the W marker layer and the thick W coating [5]. The Mo interlayer is necessary to distinguish the W marker layer from the W coating for depth profiling methods, therefore enabling the erosion of W to be measured and the quantitative determination of deposition of all elements. For the Tile 4 data presented a marker tile where the top layer is a 3 μm thick Mo (the top W layer is omitted) was used is to enable the analysis of re-deposited W.

Erosion and deposition was analysed by Ion beam Analysis (IBA) techniques using the 2.5 MV Van de Graaff accelerator installed at the Laboratory of Accelerators and Radiation Technologies of Instituto Superior Técnico. Analyses for JET were performed in a chamber dedicated to fusion research, where samples, including full JET tiles, contaminated with tritium (T) and beryllium (Be) can be handled.

Elastic Backscattering Spectrometry (EBS) and Particle Induced X-ray Emission (PIXE) were performed with 2.3 MeV incident protons. NRA using ^{3}He ions at an energy of 2.3 MeV was used to measure the amounts of ^{2}H (D), Be and C. The D(^{3}He,p)^{4}He reaction was used to measure the D content, the ^{9}Be(^{3}He,p$_{x}$)^{11}B (i = 0,1,2,3) reactions [6] for Be and ^{12}C(^{3}He,p$_{0}$)^{14}N reactions for ^{12}C. For thin deposits the NRA data provide more sensitive and accurate results for Be and C than the RBS data, which are used for thick deposits. At 2.3 MeV the NRA cross-section for carbon is very low, and in case of thick films the signal from C (^{12}C(^{3}He,p$_{0}$)^{14}N) overlaps with the Be signal (^{9}Be(^{3}He,p$_{3}$)^{11}B), limiting its detection.

The sample manipulator in the experimental chamber is fully automated and enables analysis over 150mm along the surface. This allow efficient measurement of whole JET tiles. The RBS particle detector is located at a scattering angle of 150°. The NRA detector is placed at a 135° scattering angle and has an active layer with 1 mm thickness. A 140 μm thick Al stopping foil was selected to allow the detection of D and Be protons from the ^{2}H(^{3}He,p$_{0}$)^{4}He and ^{9}Be(^{3}He,p$_{x}$)^{11}B reactions [6]. The Al foil also stops the 14 MeV α particles from ^{9}Be(^{3}He,α$_{0}$)^{8}Be reaction. Straggling in the foil does not affect the measurements since it is the signal integral that carries the information on the cross section.

The X-rays are detected by PIXE by means of a "Sirius 30" detector located at a scattering angle of 150º and a Mylar filter with 350 μm.

The tiles were scanned using EBS, RBS, NRA and PIXE, along the poloidal direction as indicated in Figure 2 for Tile 1, spectra are taken every 5 mm along the tile surface to have a complete picture of the composition.

The experimental data were analysed using the NDF code [7] to quantify all the impurities present in the tiles. The sample composition is determined in a self-consistent way with PIXE data simulated by means of LibCPIXE code [8]. The PIXE data were analysed with GUPIX code [9] and the results used as input with NDF-LibCPIXE.

3. Results

The results are presented and discussed below for each of the tiles individually.

3.1. Upper divertor (Tile 1)

On the W surface, a Be deposits with more than 10 μm thick were found at the top of Tile 1 in the region s= 162-296. It should be pointed out that thick films tend to cause proton energy dispersion, not proton particle loss, and some dispersion can be tolerated if an adjacent film barrier can be resolved; the 2.3 MeV incident protons have insufficient energy to resolve the thickness of the Be deposit without error. The EBS data together with PIXE and NRA give the concentration of the elements present in the layer. Depth profiles at each analysis point are integrated to give the concentration along the surface of Be, D, C and O in the first 5 $\times 10^{19}$ at/cm^2 of sample; over this integration depth the beam doesn't suffer large energy dispersion. These results are shown in Figure 3. These thick deposits have a complex and multi-layer structure, showing a similar pattern to the first JET-ILW campaign [2]. The concentration of Be varies from 70 % to 90%, D up to 6%, O and C from 1 % to 10%. EBS proton spectra show W and Mo at the surface, but at concentrations below 1%.

In the lower part of Tile 1 (s = 296-415 mm) a small amount of erosion of the W marker layer is likely. However due to a higher surface roughness [10] and a small deposition of Be, D, C, and O, this is difficult to quantify. A similar pattern to the first JET-ILW campaign was observed [11]. This deposition is low due to competition between deposition and erosion processes occurring in this region.

3.2. Remote inner corner (Tile 4)

Deposits rich in D, Be, C and O as well as other metals are observed on Tile 4 in the plasma shadowed surface, i.e. the flat region of the tile below the slope (s = 713-762 mm), as shown in Figure 3. On the plasma accessible surface (s = 762-934 mm), the deposit has a thickness nearly one order of magnitude lower. At the predominant strike point position s=798mm the Mo marker layer is eroded by ~40% of the nominal thickness of 3 μm, the distribution of the strike points and the Mo concentration are shown in Figures 4d and 4c respectively.

Having a Mo top surface allows W deposition to be measured. Three bands of W deposition in toroidal direction are found as shown in figure 4b, one at the top of the sloping surface (s = 840 mm), a band at the predominant strike point position (s = 800 mm) and a band in the corner of the horizontal surface (s = 772 mm). The first two bands appear to follow the strike point positions profile , the third band results probably from a re-deposition of the W on the tile or co-deposition with Be. The rest of the tile (from s≈840-934 mm), reveals a small amount of deposition, and no erosion. This deposition pattern is a little bit different than observed in the previous ILW campaign 2011-2012 [12] mainly because of changes in the strike point distribution between the campaigns.

Remote outer corner (Tile 6)

Deposition is also detected in the plasma shadowed outer corner of Tile 6 although ~5 times greater Be content than on Tile 4 and ~5 times higher than observed on Tile 6 after the 2011-2012 campaign [13]. On Tile 6 the deposition was inhomogeneous with deposition predominantly at the bottom of the sloping region in a band from s≈1430 mm to s≈1460 mm. Ni is observed in this deposit of the order of 2×10^{18} at/cm^2 due to some melting of Inconel tie rods in Tile 7. In the plasma shadowed area of Tile 6 the D, C and O are present but at lower concentrations than observed in the plasma shadowed area of Tile 4. On the upper horizontal surface of the tile (s = 1321-1429 mm) the amount of D decreases to 1-6 $\times10^{18}$ at/cm^2, the C and O are in the limit of the EBS/NRA sensitivity. This surface was partly shadowed by Tile 5 and was in the private flux region when the strike point was on tile 6. Tile 6 is a standard W coated tile, therefore it is not possible to comment where erosion occurred.

4. Conclusions

Under the present JET plasma conditions the upper divertor remains the region of highest deposition with Be rich films over 10-20 microns thick present at the top of Tile 1. Fuel retention in the deposits on Tile 1 remain similar to the 2011-2012 campaign with Be:D ratio of the order (10-15):1, typically 5.0 $\times10^{19}$ at/cm^2 of Be to 0.3 $\times10^{19}$ at/cm^2 of D in the Be rich films.

Be and D in the remote inner corner of the divertor (Tile 4) are an order of magnitude lower (~0.5 $\times10^{18}$ at/cm^2 of D) than the maximum deposition band seen at the bottom of the sloping surface (~5.0 $\times10^{18}$ at/cm^2 of D), i.e., ~5 cm beyond the main strike point. Surface analysis of the Mo marker

coating shows a W deposition in three locations: one at the predominant strike point position, one with the Be deposits and one at the top of the sloping surface.

Deposition at the outer corner of the divertor also shows a maximum deposition at the furthest region of the tile accessible by the plasma. The maximum Be deposited in this band is 3×10^{19} at./cm2, around ~5 times higher than observed in the 2011-2012 campaign for similar total time in divertor x-point plasma - 13 hours (2011-2012) compared with 14 hours (2013-2014). However the time the outer strike point was located on Tile 6 was ~ 4 times longer in 2013-2014 than in 2011-2012, which is likely to account for more material migration to this region [14].

5. Acknowledgements

This work has been carried out within the framework of the EUROfusion Consortium and has received funding from the Euratom research and training programme 2014-2018 under grant agreement No 633053. The views and opinions expressed herein do not necessarily reflect those of the European Commission. This work was also part-funded by Portuguese FCT - Fundação para a Ciência e a Tecnologia, under grant PD/BD/52411/2013 (PD-F APPLAuSE) and through project Pest-OE/SADG/LA0010/2013.

6. Reference

[1] K. Heinola, A. Widdowson, J. Likonen, E. Alves, A. Baron-Wiechec, N.P. Barradas, S. Brezinsek, N. Catarino, J.P. Coad, S. Koivuranta, S. Krat, G.F. Matthews, M. Mayer, P. Petersson, H. Maier, T. Hirai, M. Rubel, R. Neu, P. Mertens, H. Greuner, C. Hopf, G.F. Matthews, O. Neubauer, G. Piazza, E. Gauthier, J. Likonen, R. Mitteau, G. Maddaluno, B. Riccardi, V. Philipps, C. Ruset, C.P. Lungu, I. Uytdenhouwen, J.-E. Contributors, Phys. Scr. T167 (2016) 014075.

[2] A. Baron-Wiechec, A. Widdowson, E. Alves, C.F. Ayres, N.P. Barradas, S. Brezinsek, J.P. Coad, N. Catarino, K. Heinola, J. Likonen, G.F. Matthews, M. Mayer, P. Petersson, M. Rubel, W. van Renterghem, I. Uytdenhouwen, J. Nucl. Mater. 463 (2015) 157–161.

[3] A. Widdowson, E. Alves, C.F. Ayres, A. Baron-Wiechec, S. Brezinsek, N. Catarino, J.P. Coad, K. Heinola, J. Likonen, G.F. Matthews, M. Mayer, M. Rubel, Phys. Scr. T159 (2014) 014010.

[4] M. Rubel, J.P. Coad, A. Widdowson, G.F. Matthews, H.G. Esser, T. Hirai, J. Likonen, J. Linke, C.P. Lungu, M. Mayer, L. Pedrick, C. Ruset, J. Nucl. Mater. 438 (2013) S1204–S1207.

[5] C. Ruset, E. Grigore, I. Munteanu, H. Maier, H. Greuner, C. Hopf, V. Phylipps, G.F. Matthews, Fusion Eng. Des. 84 (2009) 1662–1665.

[6] N.P. Barradas, N. Catarino, R. Mateus, S. Magalhães, E. Alves, Z. Siketić, I.B. Radović, Nucl. Instruments Methods Phys. Res. Sect. B Beam Interact. with Mater. Atoms 346 (2015) 21–25.

[7] N.P. Barradas, C. Jeynes, Nucl. Instruments Methods Phys. Res. Sect. B Beam Interact. with Mater. Atoms 266 (2008) 1875–1879.

[8] C. Pascual-Izarra, N.P. Barradas, M.A. Reis, Nucl. Instruments Methods Phys. Res. Sect. B Beam Interact. with Mater. Atoms 249 (2006) 820–822.

[9] J.A. Maxwell, W.J. Teesdale, J.L. Campbell, Nucl. Instruments Methods Phys. Res. Sect. B Beam Interact. with Mater. Atoms 95 (1995) 407–421.

[10] M. Mayer, J. Likonen, J.P. Coad, H. Maier, M. Balden, S. Lindig, E. Vainonen-Ahlgren, V. Philipps, J. Nucl. Mater. 363-365 (2007) 101–106.

[11] M. Mayer, S. Krat, W. Van Renterghem, A. Baron-Wiechec, S. Brezinsek, I. Bykov, J.P. Coad, Y. Gasparyan, K. Heinola, J. Likonen, A. Pisarev, C. Ruset, G. de Saint-Aubin, A. Widdowson, H. Maier, T. Hirai, M. Rubel, R. Neu, P. Mertens, H. Greuner, C. Hopf, G.F. Matthews, O. Neubauer, G. Piazza, E. Gauthier, J. Likonen, R. Mitteau, G. Maddaluno, B. Riccardi, V. Philipps, C. Ruset, C.P. Lungu, I. Uytdenhouwen, J.-E. Contributors, Phys. Scr. 2016 (2016) 14051.

[12] K. Heinola, A. Widdowson, J. Likonen, E. Alves, A. Baron-Wiechec, N.P. Barradas, S. Brezinsek, N. Catarino, J.P. Coad, S. Koivuranta, G.F. Matthews, M. Mayer, P. Petersson, J. Nucl. Mater. 463 (2015) 961–965.

[13] P. Petersson, M. Rubel, H.G. Esser, J. Likonen, S. Koivuranta, A. Widdowson, J. Nucl. Mater. 463 (2015) 814–817.

[14] A. Widdowson, E. Alves, A. Baron-Wiechec, N.P. Barradas, N. Catarino, J.P. Coad, V. Corregidor, A. Garcia-Carrasco, K. Heinola, S. Koivuranta, S. Krat, A. Lahtinen, J. Likonen, M. Mayer, P. Petersson, S. van Boxel, Nucl. Mater. Energy (n.d.) These Proceedings.

Figure caption

Fig.1. JET divertor during the JET-ILW campaign 2013 to 2014. The s-coordinate (in mm) starts at the upper left corner of Tile 0 and follows the tile surfaces. In blue the tiles studied in this paper, the Tile 1 apron is between s-coordinates 162 mm and 431 mm, Tile 4 between s-coordinates 413 mm and 934 mm and Tile 6 between s-coordinates 1321 mm and 1510 mm.

Fig. 2. Schematic view of a marker Tile 1. Due to the tile geometry three analysis scans were made as indicated in the diagram, in order to minimize the effect of the angle between the sample normal and the direction of the incident beam.

Fig.3. Total deposition of Be, D, C and O on the marker tiles. The concentration for Tile 1 is the integrated concentration in the first 5×10^{19} at/cm^2 of sample.

Fig.4. Tile 4 (a) s-coordinate between 413 mm and 934, showing the regions referred to in the text. (b) Integration of W concentration in the first 10^{19} at/cm^2 of the tile surface (i.e. deposited on top of the marker) (c) Total concentration of the Mo marker layer, and (d) a histogram of strike point positions for the JET-ILW campaign 2013 to 2014.

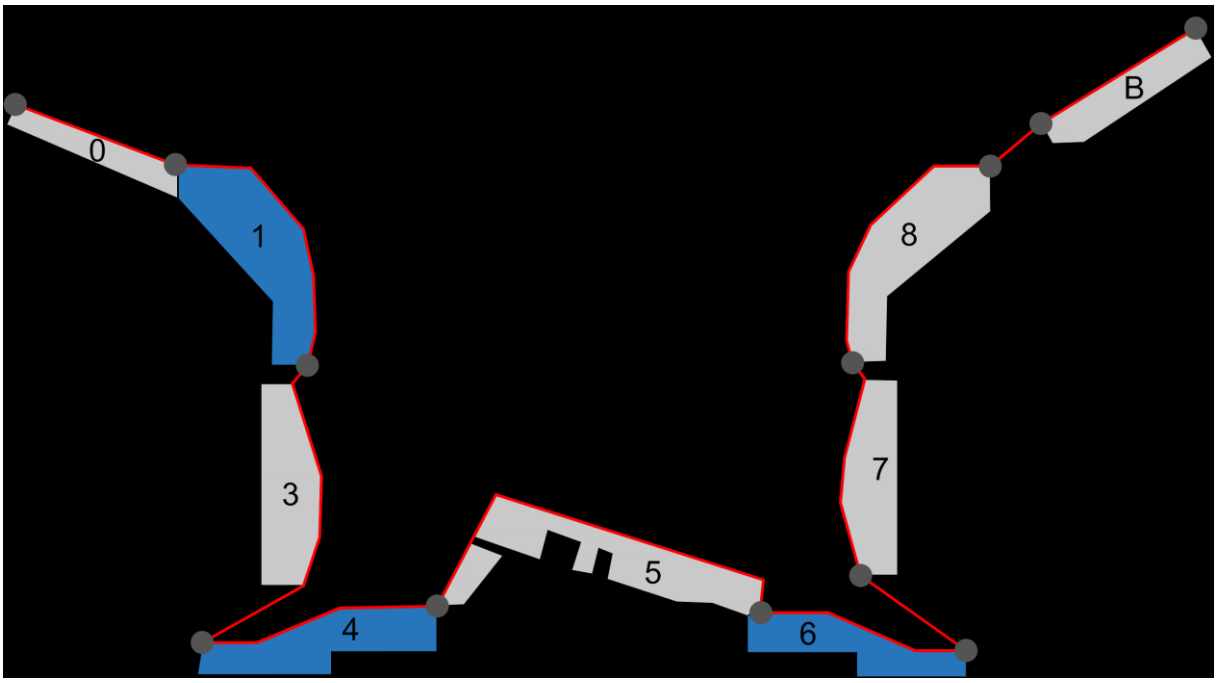

Fig.1.

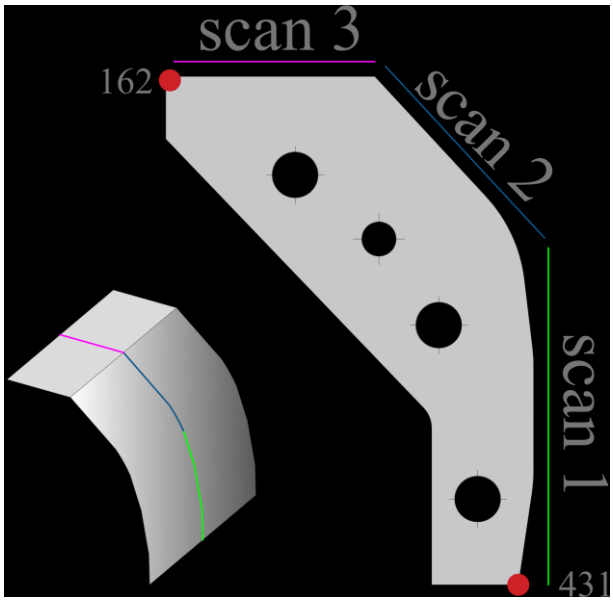

Fig.2.

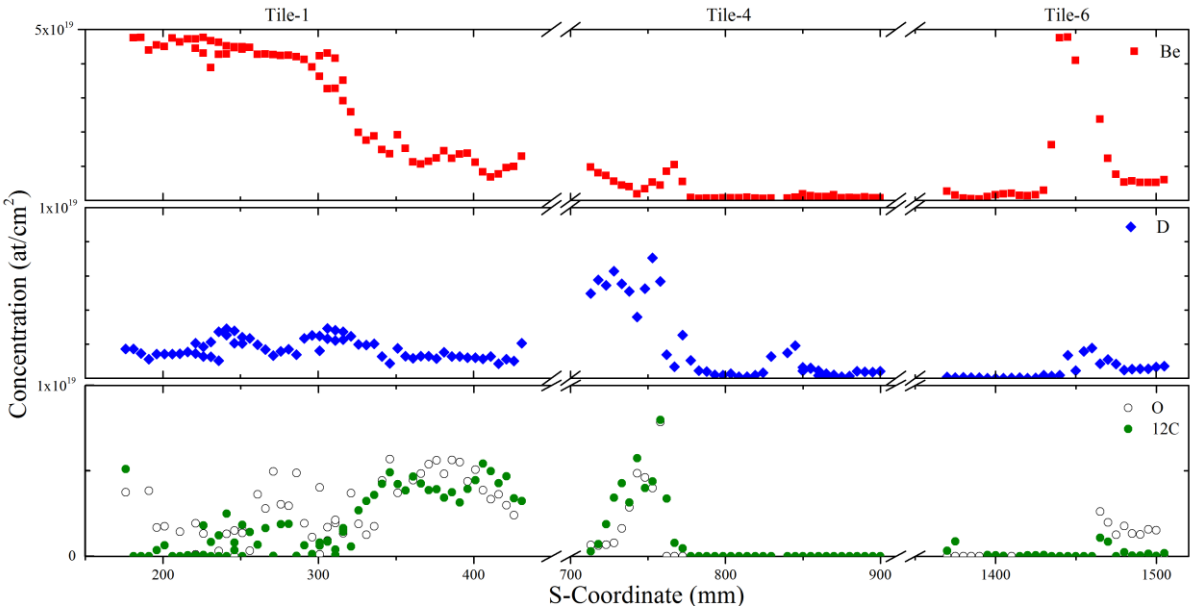
Tile-1
Tile-4
Tile-6
Be
D
O
12C
Concentration (at/cm^2)
S-Coordinate (mm)

Fig.3.

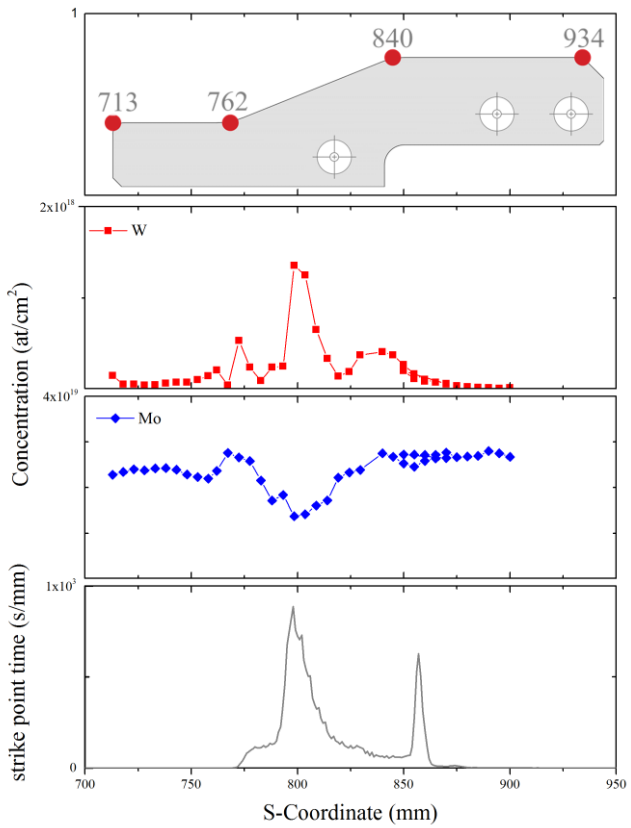
840
934
713
762
W
Mo
Concentration (at/cm^2)
strike point time (s/mm)
S-Coordinate (mm)

Fig.4.